Malignant oligoastrocytoma in the spinal cord of a cat

Dai HASEGAWA[1], Keisuke AOSHIMA[1]*, Kazuyoshi SASAOKA[2],
Atsushi KOBAYASHI[1], Mitsuyoshi TAKIGUCHI[3], Takashi KIMURA[1]

[1] Laboratories of Comparative Pathology, Department of Clinical Sciences, Faculty of Veterinary Medicine, Hokkaido University, Hokkaido, Japan
[2] Veterinary Teaching Hospital, Faculty of Veterinary Medicine, Hokkaido University, Hokkaido, Japan
[3] Veterinary Internal Medicine, Department of Clinical Sciences, Faculty of Veterinary Medicine, Hokkaido University, Hokkaido, Japan

ABSTRACT. A 12-year and 3-month spayed female mixed cat was presented with severe lumbar pain. Magnetic resonance imaging and postmortem examination revealed a swollen lesion in the spinal cord at L3 level. Histologic examination identified extensive neoplastic cell proliferation with massive necrosis in the tumor tissue. Two types of neoplastic cells were recognized. One type of neoplastic cells were large cells characterized by round to polygonal shape and abundant eosinophilic cytoplasm (referred to as "large cells"). The other neoplastic cells were small, densely proliferated, and had round to irregular shape and scant eosinophilic cytoplasm (referred to as "small cells"). Both types of cells were positive for oligodendrocyte transcription factor 2 and SRY-box transcription factor 10. Glial fibrillary acidic protein was positive in large cells but negative in most small cells. Digital analysis for Ki-67-stained tumor tissues found that total 21.1% ± 6.5% of tumor cells were positive for Ki-67. Based on these findings, we diagnosed malignant oligoastrocytoma in the spinal cord.

KEYWORDS: cat, Ki-67, oligoastrocytoma, spinal cord, tumor

Spinal cord tumors are classified based on their location: extradural, intradural-extraparenchymal, or intraparenchymal. The most common tumor in the spinal cord of cats is malignant lymphoma, which can develop in any of the location [16, 17]. Intraparenchymal tumors in the spinal cord of cats are rare. One study has reported that 8 out of 85 spinal cord tumors were intraparenchymal, and only a few case reports of intraparenchymal spinal cord tumors have been published [8, 18, 23]. One study summarizing intraparenchymal spinal cord tumors in cats has shown several types of gliomas such as astrocytoma, oligodendroglioma, oligoastrocytoma and gliomatosis cerebri [7]. Although the number of cases studied in the report was small, most of the tumors were developed in either the cervical or thoracic regions [7]. Here we report a feline case of malignant oligoastrocytoma in the lumbar spinal cord.

A 12-year and 3-month spayed female mixed breed cat was presented to a local veterinary hospital because of severe lumbar pain on Mar. 2nd, 2021. Decreased postural reactions in the hindlimbs and dysuria were observed. The cat was placed on prednisolone and cartrophen because intervertebral disc herniation was suspected; however, the cat failed to respond to treatment and was referred to Hokkaido University Veterinary Teaching Hospital (HUVTH) on Mar. 23rd, 2021. At presentation at HUVTH, the cat had hindlimb paralysis and loss of deep pain sensation. Magnetic resonance imaging (MRI) revealed a mass lesion in the spinal cord at L3 level (Fig. 1A). No abnormalities were detected in cerebrospinal fluid analysis (protein concentration: 30 mg/dL, total nucleated cell count: 0 cell/μL, erythrocytes: 31 cells/μL). Pain relief treatment was continued, but the cat did not respond to it. At the owner's request, the cat was euthanized on Apr. 20th, 2021. Postmortem examination was performed three hours after euthanasia.

Grossly, the left part of the spinal cord from L3 to L4 level was moderately swollen over a 3.0 cm long × 0.5 cm wide area, and the lesion was slightly dark pale pink to pale brown in color (Fig. 1B). The cut surface of the lesion was homogenously pale tan, and the boundary between the white and gray matter was obscure. In addition to the spinal cord lesion, muscle atrophy in both hind limbs and bladder calculi were observed.

We collected and fixed the tumor samples from the spinal cord in 10% neutral buffered formalin. Then, the tissues were dehydrated, cleared, and infiltrated with ethanol, xylene, and paraffin wax, respectively. Afterwards, the tissues were embedded in paraffin blocks, sliced into 2 μm thickness, and subject to hematoxylin and eosin staining or immunohistochemical staining. For immunohistochemistry,
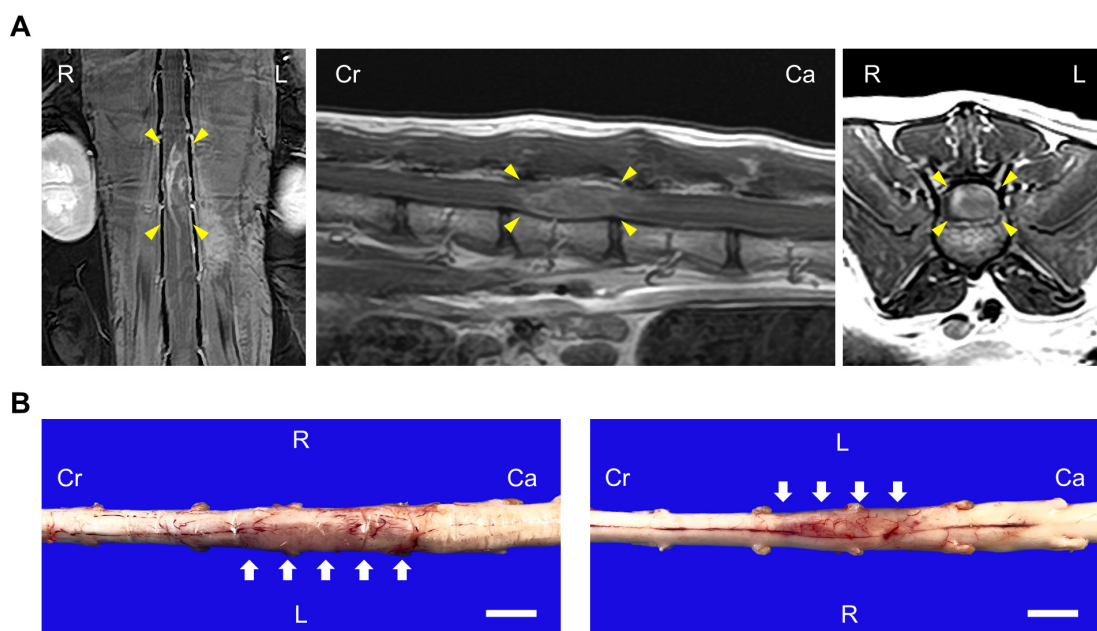
Fig. 1. MRI and gross images of the lumbar spinal cord. (**A**) T1-weighed MRI planes of the spinal cord following contrast administration. Arrow heads indicate the mass lesion. Left: coronal. Middle: sagittal. Right: axial. (**B**) Gross images of dorsal (left) and ventral (right) side of the spinal cord. Arrows indicate the swollen lesion. Bars=1 cm. R=right, L=left, Cr=cranial, Ca=caudal.

endogenous peroxidase was inactivated with 0.3% H_2O_2 in methanol. Blocking and antibody staining were done using Histofine Simple Stain Kit (Nichirei, Tokyo, Japan. 424134 or 424144) according to the manufacturer's instructions. Signals were developed by reaction with 3.3′-diaminobenzidine (DAB: Dojindo, Kumamoto, Japan. 349-00903). Primary antibodies used in this study and antibody retrieval methods were summarized in Table 1. They were validated for use in cats either by positive control staining or by other researchers or both (Supplementary Fig. 1 and Table 1) [9, 11, 20]. For quantitative analysis, stained slides were digitally scanned with NanoZoomer 2.0-RS (Hamamatsu Photonics, Hamamatsu, Japan) and analyzed with QuPath ver 2.1.0 [2]. The whole tumor area was analyzed for oligodendrocyte transcription factor 2 (OLIG2) and SRY-box transcription factor 10 (SOX10). For glial fibrillary acidic protein (GFAP), partial tumor areas with high staining resolution and clear cell segmentation were selected for accurate analysis because GFAP expressed both in the cytoplasm of tumor cells and reactive astrocytes within the tumor tissues. Large tumor cells and reactive astrocytes were differentially classified by GFAP staining intensity and nuclear/cytoplasmic morphology during annotation. For Ki-67, 10 randomly selected areas in the tumor tissue were analyzed considering heterogenous proliferation patterns of tumor cells. DAB OD mean value was used as intensity. Threshold intensities for positive/negative sub-classification were 0.1 for OLIG2 and SOX10, 0.07 for GFAP, and 0.23 for Ki-67 based on the staining appearance and intensity histograms. The Mann-whitney U test was performed to analyze statistical differences using R ver. 3.6.3.

Histologically, an unencapsulated poorly demarcated tumor mass was located in the parenchyma of the swollen lesion in the spinal cord (Fig. 2A). Massive necrosis was observed in the central area around which tumor cells extensively proliferated, leading to compression of the adjacent normal tissue. In higher magnification, two types of morphologically different neoplastic cells were recognized. One was large neoplastic cells characterized by round to polygonal shape and abundant eosinophilic cytoplasm (hereinafter referred to as "large cells") (Fig. 2B). The other neoplastic cells were small, densely proliferated, and had round to irregular shape and scant eosinophilic cytoplasm (hereinafter referred to as "small cells") (Fig. 2C). Both neoplastic cells possessed round to oval clear nuclei with one or two distinct nucleoli, but large cells occasionally had irregularly shaped nuclei and cytoplasm. Although both large and small cells showed marked anisokaryosis and anisocytosis, mitotic figures were found more frequently in small cells than in large cells. Quantitative analysis revealed that small cells had 355 mitotic figures out of 12,838 cells (2.8%) while large cells exhibited 30 mitotic figures out of 9,642 cells (0.3%). Mitotic activity indices by manual counting were 17 per 10 high power fields (HPF) (2.37 mm^2) in small cells and 2 per 10 HPF in large cells. Each cell type was equally intermingled in the most part of the tumor tissues although either cell type was slightly dominant in some areas. Newly formed blood vessels surrounded by neoplastic cells were observed throughout the tumor tissues (Fig. 2D). No glomeruloid vascular proliferation, the characteristic neovascularization in malignant glioma, was observed. Reactive astrocytes and microglia were scattered in the tumor tissues and adjacent tissues.

Immunohistochemical analyses revealed that both large and small cells were positive for OLIG2 and SOX10, pivotal transcription factors for oligodendrocyte differentiation [12, 15, 24, 26], and that OLIG2 expressed higher in large cells than small cells but SOX10 showed the opposite result (Fig. 3A–3D, Table 2). Large cells showed weak to moderate positivity for an astrocyte marker GFAP, but most small cells were negative for GFAP (Fig. 3E and 3F). Tumor cells had no positive signal for ionized calcium binding adaptor molecule 1 (IBA1) and beta III tubulin, a microglia marker and a neuron marker, respectively, and in PBS controls (Supplementary

Table 1. Antibody information

Target	Clone	Maker	Catalog #	Antigen retrieval method	Reference
GFAP	Polyclonal	Agilent Technologies, Santa Clara CA, USA	Z0334	Tris-EDTA buffer (pH9.0) in a microwave, 15 min	[9]
OLIG2	Polyclonal	MilliporeSigma, Burlington, MA, USA	AB9610	Citrate buffer (pH6.0) in a pressure cooker, 15 min	[17]
SOX10	E6B6I	Cell Signaling Technology, Danvers, MA, USA	69661S	Citrate buffer (pH6.0) in a microwave, 15 min	-
IBA1	Polyclonal	FUJIFILM Wako, Osaka, Japan	019-19741	Citrate buffer (pH6.0) in a pressure cooker, 15 min	[7]
Beta III tubulin	TU-20	MilliporeSigma	MAB1637	Citrate buffer (pH6.0) in a microwave, 15 min	-
Ki-67	MIB-1	Agilent Technologies	GA626	Tris-EDTA buffer (pH9.0) in a pressure cooker, 15 min	-

GFAP: glial fibrillary acidic protein; OLIG2: oligodendrocyte transcription factor 2; SOX10: SRY-box transcription factor 10; IBA1: ionized calcium binding adaptor molecule 1; EDTA: ethylenediaminetetraacetic acid.
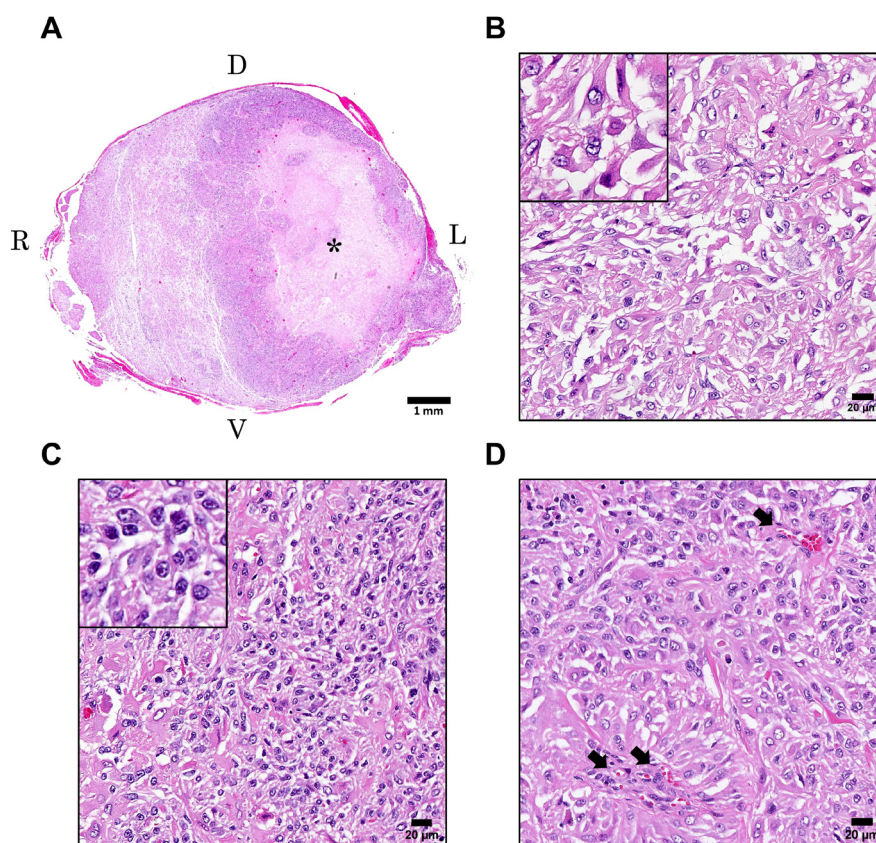

Fig. 2. Hematoxylin and eosin staining of the mass in the lumbar spinal cord. (**A**) The subgross image of the lumbar spinal cord. The asterisk indicates the necrotic area. (**B–D**) High magnification of the tumor tissues. Insets show large cells (B) and small cells (C). Arrows in D indicate newly formed blood vessels. D=dorsal, V=ventral, R=right, L=left. Scale bars=1 mm (A), 20 µm (B–D).

Fig. 2). To measure the mitotic activity of tumor cells quantitatively, Ki-67 staining was performed in 10 randomly selected areas in the tumor tissue, each of which contained at least 400 each of large and small cells. Total $21.1 \pm 6.5\%$ of tumor cells were positive for Ki-67, out of which $3.1 \pm 1.0\%$ were large cells and $18.0 \pm 6.4\%$ were small cells (Fig. 3G and 3H). Calculations within each tumor cell type indicated that $8.6 \pm 3.1\%$ of large cells and $29.2 \pm 5.6\%$ of small cells were positive for Ki-67 (Fig. 3I).

In the present case, we detected two types of neoplastic cells equally admixing in the tumor tissues: large and small cells. Large cells had astrocyte-like characteristics such as pleomorphism, abundant eosinophilic cytoplasm and GFAP positivity. On the other hand, small cells showed oligodendrocyte-like characteristics such as scant cytoplasm, dense proliferation and GFAP negativity although perinuclear halo, a typical oligodendroglioma cell feature, was not detected. On top of that, both cell types possessed
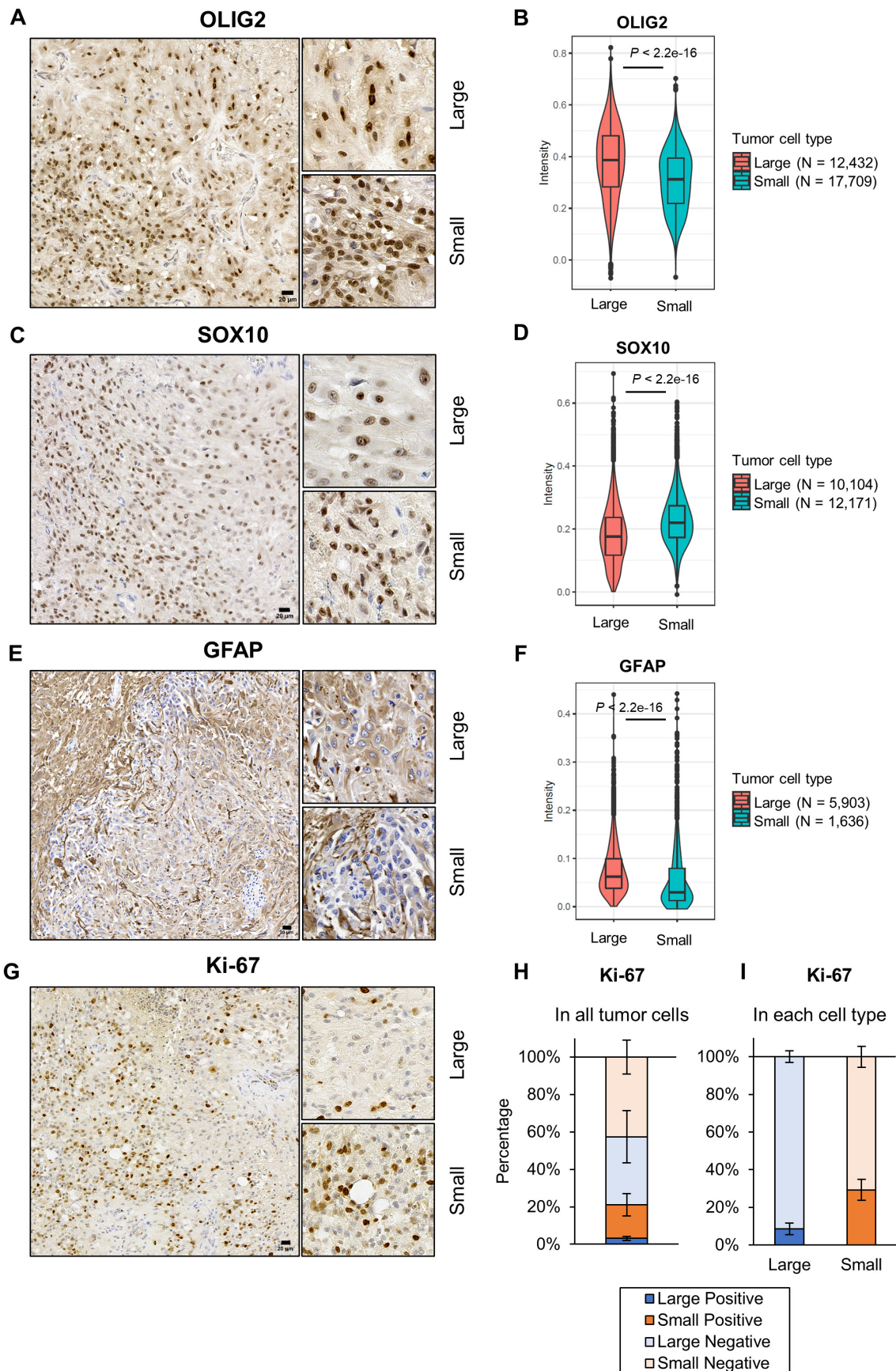
Fig. 3. Immunohistochemistry of the mass in the lumbar spinal cord. (**A–F**) Representative images (A, C, E) and signal intensities (B, D, F) of oligodendrocyte transcription factor 2 (OLIG2), SRY-box transcription factor 10 (SOX10) and glial fibrillary acidic protein (GFAP) staining. (**G**) Representative images of Ki-67. (**H** and **I**) Ki-67 expression profiles in all tumor cells (H) and in each tumor cell type (I). The graphs were created based on the average percentages ± SD. Large=large cells, Small=small cells. Bars=20 μm.

Table 2. Immunihitochemical characteristics of tumor cells

Protein	Cell type	Total number of analyzed cells	Number of positive cells	Percentage of positive cells
OLIG2	Large cells	12,432	12,114	97.4
	Small cells	17,709	17,265	97.5
SOX10	Large cells	10,104	8,120	80.4
	Small cells	12,171	11,729	96.4
GFAP	Large cells	5,903	4,320	73.2
	Small cells	1,636	452	27.6

malignant features such as marked anisokaryosis and anisocytosis, and small cells had high mitotic rates. These findings suggest that this tumor was composed of astrocytic and oligodendrocytic neoplastic cells almost at the same rate; thus, we diagnosed malignant oligoastrocytoma in the spinal cord.

Oligoastrocytoma is composed of mixed neoplastic populations [22]. It is an uncommon tumor in cats and a few cases have been reported in the brain or spinal cord [7, 21]. Immunohistochemistry is useful to identify tumor cell types; however, there are some issues on it. OLIG2 is an important transcription factor for oligodendrocyte differentiation, but several recent studies demonstrated that astrocytoma can also be positive for OLIG2 in dogs, cats and humans [10, 14]. When tumor cells are negative for GFAP, OLIG2 is useful as a marker for oligodendroglial tumors [10]. SOX10, another transcription factor driving oligodendrocyte differentiation, has also been reported to be detected in human astrocytoma although there has been no systematic study investigating SOX10 positivity in astrocytoma in dogs and cats [5]. In the present case, both large and small cells were positive for OLIG2 and SOX10, but only large cells were positive for GFAP. In human cases, SOX10 expression is lower in tumors showing astrocytic phenotype than those showing oligodendrocytic phenotype [3], which led us to a speculation that large cells have astrocytic phenotype and small cells have oligodendrocytic phenotype.

Mitotic figure counting and Ki-67 staining revealed that small cells were more actively proliferating than large cells. One hypothesis explaining this is that small cells are more undifferentiated than large cells. Given that astrocytes can be differentiated from OLIG2-positive cells [4, 19], large cells might be derived from small cells. Another possibility is that small cells simply have the propensity to proliferate more actively than large cells regardless of their differentiation status. However, the exact reason why small cells showed high proliferation activity remains unknown.

Ki-67 labeling index (LI) is a conventional way to evaluate the mitotic activity of tumor cells, which has been widely used to assess tumor malignancy [13]. However, interobserver variability has been proposed as a concern [1, 6]. Advanced digital technologies such as virtual slides and image analysis software allowed us to count Ki-67 LI in a more objective way [1]. Digital analysis can provide high interoperator reproducibility and makes it possible to evaluate larger areas, even whole slides, than analog analysis [1, 25]. In this report, we randomly selected 10 areas of the tumor tissue considering heterogeneous neoplastic cell proliferation patterns. Guidelines for digital analysis should be established for each tumor type to accomplish high reproducibility and a better evaluation of tumor malignancy.

In summary, we reported a feline spinal cord malignant oligoastrocytoma case and utilized digital image analysis technique to quantitatively evaluate protein expression levels and Ki-67 LI on pathology slides. Given that spinal cord glioma in cats is uncommon, accumulating case data is highly warranted to further understand its pathogenesis.

REFERENCES

1. Acs B, Pelekanou V, Bai Y, Martinez-Morilla S, Toki M, Leung SCY, Nielsen TO, Rimm DL. 2019. Ki67 reproducibility using digital image analysis: an inter-platform and inter-operator study. *Lab Invest* **99**: 107–117. [Medline] [CrossRef]
2. Bankhead P, Loughrey MB, Fernández JA, Dombrowski Y, McArt DG, Dunne PD, McQuaid S, Gray RT, Murray LJ, Coleman HG, James JA, Salto-Tellez M, Hamilton PW. 2017. QuPath: Open source software for digital pathology image analysis. *Sci Rep* **7**: 16878. [Medline] [CrossRef]
3. Bannykh SI, Stolt CC, Kim J, Perry A, Wegner M. 2006. Oligodendroglial-specific transcriptional factor SOX10 is ubiquitously expressed in human gliomas. *J Neurooncol* **76**: 115–127. [Medline] [CrossRef]
4. Dimou L, Simon C, Kirchhoff F, Takebayashi H, Götz M. 2008. Progeny of Olig2-expressing progenitors in the gray and white matter of the adult mouse cerebral cortex. *J Neurosci* **28**: 10434–10442. [Medline] [CrossRef]
5. Ferletta M, Uhrbom L, Olofsson T, Pontén F, Westermark B. 2007. Sox10 has a broad expression pattern in gliomas and enhances platelet-derived growth factor-B—induced gliomagenesis. *Mol Cancer Res* **5**: 891–897. [Medline] [CrossRef]
6. Grzybicki DM, Liu Y, Moore SA, Brown HG, Silverman JF, D'Amico F, Raab SS. 2001. Interobserver variability associated with the MIB-1 labeling

index: high levels suggest limited prognostic usefulness for patients with primary brain tumors. *Cancer* **92**: 2720–2726. [Medline] [CrossRef]

7. Hammond JJ, deLahunta A, Glass EN, Kent M, Summers BA, Miller AD. 2014. Feline spinal cord gliomas: Clinicopathologic and diagnostic features of seven cases. *J Vet Diagn Invest* **26**: 513–520. [Medline] [CrossRef]

8. Haynes JS, Leininger JR. 1982. A glioma in the spinal cord of a cat. *Vet Pathol* **19**: 713–715. [Medline] [CrossRef]

9. Ide T, Uchida K, Tamura S, Nakayama H. 2010. Histiocytic sarcoma in the brain of a cat. *J Vet Med Sci* **72**: 99–102. [Medline] [CrossRef]

10. Johnson GC, Coates JR, Wininger F. 2014. Diagnostic immunohistochemistry of canine and feline intracalvarial tumors in the age of brain biopsies. *Vet Pathol* **51**: 146–160. [Medline] [CrossRef]

11. Keating MK, Sturges BK, Sisó S, Wisner ER, Creighton EK, Lyons LA. 2016. Characterization of an inherited neurologic syndrome in toyger cats with forebrain commissural malformations, ventriculomegaly and interhemispheric cysts. *J Vet Intern Med* **30**: 617–626. [Medline] [CrossRef]

12. Kuhlbrodt K, Herbarth B, Sock E, Hermans-Borgmeyer I, Wegner M. 1998. Sox10, a novel transcriptional modulator in glial cells. *J Neurosci* **18**: 237–250. [Medline] [CrossRef]

13. Li LT, Jiang G, Chen Q, Zheng JN. 2015. Ki67 is a promising molecular target in the diagnosis of cancer (review). *Mol Med Rep* **11**: 1566–1572. [Medline] [CrossRef]

14. Ligon KL, Alberta JA, Kho AT, Weiss J, Kwaan MR, Nutt CL, Louis DN, Stiles CD, Rowitch DH. 2004. The oligodendroglial lineage marker OLIG2 is universally expressed in diffuse gliomas. *J Neuropathol Exp Neurol* **63**: 499–509. [Medline] [CrossRef]

15. Lu QR, Sun T, Zhu Z, Ma N, Garcia M, Stiles CD, Rowitch DH. 2002. Common developmental requirement for Olig function indicates a motor neuron/oligodendrocyte connection. *Cell* **109**: 75–86. [Medline] [CrossRef]

16. Mandara MT, Motta L, Calò P. 2016. Distribution of feline lymphoma in the central and peripheral nervous systems. *Vet J* **216**: 109–116. [Medline] [CrossRef]

17. Marioni-Henry K, Vite CH, Newton AL, Van Winkle TJ. 2004. Prevalence of diseases of the spinal cord of cats. *J Vet Intern Med* **18**: 851–858. [Medline] [CrossRef]

18. Marioni-Henry K, Van Winkle TJ, Smith SH, Vite CH. 2008. Tumors affecting the spinal cord of cats: 85 cases (1980–2005). *J Am Vet Med Assoc* **232**: 237–243. [Medline] [CrossRef]

19. Masahira N, Takebayashi H, Ono K, Watanabe K, Ding L, Furusho M, Ogawa Y, Nabeshima Y, Alvarez-Buylla A, Shimizu K, Ikenaka K. 2006. Olig2-positive progenitors in the embryonic spinal cord give rise not only to motoneurons and oligodendrocytes, but also to a subset of astrocytes and ependymal cells. *Dev Biol* **293**: 358–369. [Medline] [CrossRef]

20. Oikawa K, Teixeira LBC, Keikhosravi A, Eliceiri KW, McLellan GJ. 2021. Microstructure and resident cell-types of the feline optic nerve head resemble that of humans. *Exp Eye Res* **202**: 108315. [Medline] [CrossRef]

21. Rissi DR, Miller AD. 2017. Feline glioma: a retrospective study and review of the literature. *J Feline Med Surg* **19**: 1307–1314. [Medline] [CrossRef]

22. Shimizu T, Saito N, Aihara M, Kurihara H, Nakazato Y, Ueki K, Sasaki T. 2004. Primary spinal oligoastrocytoma: a case report. *Surg Neurol* **61**: 77–81, discussion 81. [Medline] [CrossRef]

23. Stigen O, Ytrehus B, Eggertsdottir AV. 2001. Spinal cord astrocytoma in a cat. *J Small Anim Pract* **42**: 306–310. [Medline] [CrossRef]

24. Stolt CC, Rehberg S, Ader M, Lommes P, Riethmacher D, Schachner M, Bartsch U, Wegner M. 2002. Terminal differentiation of myelin-forming oligodendrocytes depends on the transcription factor Sox10. *Genes Dev* **16**: 165–170. [Medline] [CrossRef]

25. Zarella MD, Bowman D, Aeffner F, Farahani N, Xthona A, Absar SF, Parwani A, Bui M, Hartman DJ. 2019. A practical guide to whole slide imaging a white paper from the digital pathology association. *Arch Pathol Lab Med* **143**: 222–234. [Medline] [CrossRef]

26. Zhou Q, Anderson DJ. 2002. The bHLH transcription factors OLIG2 and OLIG1 couple neuronal and glial subtype specification. *Cell* **109**: 61–73. [Medline] [CrossRef]